Design Proposal: Mach–Zehnder Interferometers

Prasad Hardas, prahardas@gmail.com

Abstract

This design proposal presents a series of Mach–Zehnder interferometer (MZI) circuits to extract the group index of 220 nm-thick SOI waveguides. The designs use a fixed waveguide geometry (500 nm-wide quasi-TE strip) and vary the path length difference ΔL between the interferometer arms, and replicate one geometry to study the impact of fabrication process variations. The compact models for the effective and group indices are developed from mode simulations. The analytical transfer functions were used to predict the transmission spectra and free spectral range (FSR) of the interferometers.

I. Introduction

Silicon photonics has become a leading platform for integrated optics because of high index contrast, compact device footprints, and compatibility with CMOS fabrication processes [1], [4]. By integrating waveguides, splitters, couplers and resonant structures on a single chip, it is possible to implement complex optical signal-processing functions for communications, sensing and computing.

Interferometric circuits such as Mach–Zehnder interferometers (MZIs) are key building blocks in many of these systems. They are widely used for modulation, filtering and sensing, and their operation relies on the coherent interference of optical fields that have accumulated different phases along distinct paths [2], [3].

In this design project, several unbalanced Mach–Zehnder interferometers (MZIs) were designed based on 220 nm-thick silicon strip waveguides to enable extraction of the waveguide group index from the measured free spectral range (FSR). All circuits use a 500 nm-wide waveguide and quasi-TE polarization; the path length difference ΔL between the arms is varied, and one design is duplicated in two locations to quantify fabrication and process variability.

II. Theory

In this section, the basic theory and compact equations used in the design and simulation of Mach–Zehnder interferometers (MZIs) are summarized. The goal is not to provide detailed derivations, but rather to define the key building blocks and formulae that will be used later for modeling, simulation, and data analysis. The notation and concepts follow standard photonics texts such as [1], [2], [3].

A. Effective and Group Index

For a guided mode with effective index $n_{\text{eff}}(\lambda)$, the propagation constant is

$$\beta(\lambda) = \frac{2\pi}{\lambda} n_{\text{eff}}(\lambda). \tag{1}$$

The group index is defined as

$$n_g(\lambda) = n_{\text{eff}}(\lambda) - \lambda \frac{dn_{\text{eff}}}{d\lambda}. \tag{2}$$

To obtain a compact model for use in circuit simulations, we approximate $n_{\text{eff}}(\lambda)$ near a reference wavelength λ_0 as a low-order polynomial

$$n_{\text{eff}}(\lambda) \approx a_0 + a_1(\lambda - \lambda_0) + a_2(\lambda - \lambda_0)^2, \tag{3}$$

where a_0, a_1, and a_2 are obtained by least-squares fitting to mode solver data. Differentiating (3) and substituting into (2) gives

$$\frac{dn_{\text{eff}}}{d\lambda} \approx a_1 + 2a_2(\lambda - \lambda_0), \tag{4}$$

$$n_g(\lambda) \approx n_{\text{eff}}(\lambda) - \lambda \left[a_1 + 2a_2(\lambda - \lambda_0) \right]. \tag{5}$$

These expressions provide a compact model for both n_{eff} and n_g suitable for use in MATLAB or Lumerical INTERCONNECT.

B. MZI Transfer Function

We consider an unbalanced MZI formed by two nominally identical 50/50 Y-branch splitters and two arms of length L_1 and $L_2 = L_1 + \Delta L$. Neglecting loss imbalance, the phase difference between the two arms is

$$\Delta\phi(\lambda) = \beta(\lambda)\Delta L = \frac{2\pi}{\lambda}n_{\text{eff}}(\lambda)\Delta L. \tag{6}$$

For ideal 3 dB splitters, the normalized intensity transmission at one output port is

$$T(\lambda) = \frac{1}{2}\left[1 + \cos\left(\Delta\phi(\lambda)\right)\right]. \tag{7}$$

In practice, finite extinction ratio and splitter imbalance can be captured by introducing a visibility factor $0 \leq V \leq 1$ and a static phase offset ϕ_0,

$$T(\lambda) = T_0\left[1 + V\cos\left(\Delta\phi(\lambda) + \phi_0\right)\right], \tag{8}$$

where T_0 accounts for insertion loss. In the present proposal, we use (7) as the ideal transfer function for analytical simulations and will refine the visibility and offset parameters after measurements.

C. Group Index from Free Spectral Range

Constructive interference occurs when

$$\Delta\phi(\lambda_m) = \beta(\lambda_m)\Delta L = 2\pi m, \tag{9}$$

for integer m. The next maximum at $\lambda_{m+1} = \lambda_m + \Delta\lambda_{\text{FSR}}$ satisfies

$$\Delta\phi(\lambda_{m+1}) = \beta(\lambda_{m+1})\Delta L = 2\pi(m+1). \tag{10}$$

Subtracting and assuming $\Delta\lambda_{\text{FSR}}$ is small,

$$\left[\beta(\lambda_{m+1}) - \beta(\lambda_m)\right]\Delta L \approx 2\pi. \tag{11}$$

Using a first-order Taylor expansion,

$$\left.\frac{d\beta}{d\lambda}\right|_{\lambda_0}\Delta\lambda_{\text{FSR}}\,\Delta L \approx 2\pi. \tag{12}$$

From dispersion theory,

$$n_g = c\frac{d\beta}{d\omega}, \tag{13}$$

and, after transforming from frequency to wavelength and rearranging (12), we obtain the familiar wavelength-domain expression

$$\Delta\lambda_{\text{FSR}} \approx \frac{\lambda_0^2}{n_g(\lambda_0)\,\Delta L}, \tag{14}$$

or equivalently

$$n_g(\lambda_0) \approx \frac{\lambda_0^2}{\Delta\lambda_{\text{FSR}}\,\Delta L}. \tag{15}$$

In this work, the equation (14) was used to extract the FSR values from simulated waveguide group index. Experimentally, the FSR will be obtained by measuring the wavelength spacing between adjacent maxima (or minima) in the transmission spectrum and compared with computed values.
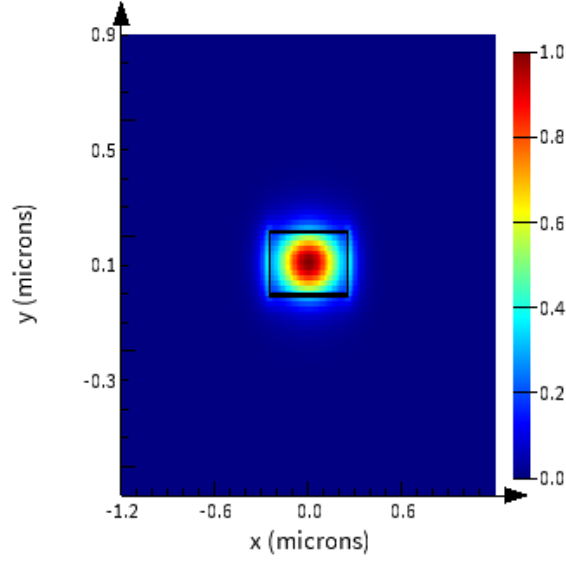
Fig. 1. Simulated fundamental TE mode profile for a $500\,\text{nm} \times 220\,\text{nm}$ silicon strip waveguide at $1550\,\text{nm}$.

III. MODELLING AND SIMULATION

A. Waveguide Geometry and Mode Profiles

All designs are implemented on a silicon-on-insulator platform with a silicon device layer thickness of 220 nm and a buried oxide cladding. The waveguide geometry is fixed to a single-mode strip with width $W = 500\,\text{nm}$, optimized for the fundamental quasi-TE mode near $\lambda_0 = 1550\,\text{nm}$. Fibre grating couplers and other passive components will be selected from the provided PDK for TE polarization.

The fundamental TE mode profile for the 500 nm $\times$ 220 nm waveguide was simulated using Lumerical MODE Solutions and the resulting electric field magnitude plot is shown in Fig. 1.

B. Effective and Group Index vs. Wavelength

For the 500 nm-wide waveguide, the effective index $n_{\text{eff}}(\lambda)$ were computed over a wavelength range of 1500–1600 nm using the mode solver. The resulting $n_{\text{eff}}(\lambda)$ curve were fitted to the polynomial model in (3), and the corresponding group index $n_g(\lambda)$ were obtained using (2).

Figure 2 shows the simulated group index as a function of wavelength for the TE strip. Figure 3 shows the simulated effective index as a function of wavelength for the TE strip, together with the polynomial fit. The obtained fit model by running script was

$$n_{\text{eff}}(\lambda) \approx 2.443 - 1.131(\lambda - 1.55) - 0.0426(\lambda - 1.55)^2, \tag{16}$$

C. Interferometer Designs and Parameter Variations

The proposal focuses on five MZI designs, all using the same 500 nm-wide TE strip waveguide and Y-branch splitters. The only varying parameter is the path length difference ΔL; one design is duplicated to study fabrication variability. Table I summarizes the interferometer designs and calucalted FSR at $1550\,\text{nm}$ with $n_g = 4.197$ calculated using (15)

D. Transmission Spectra

The transmission spectra of the interferometers were computed using the analytical transfer function in (7) together with the compact model for $n_{\text{eff}}(\lambda)$, and cross-checked using circuit-level simulations in Lumerical IN-TERCONNECT.
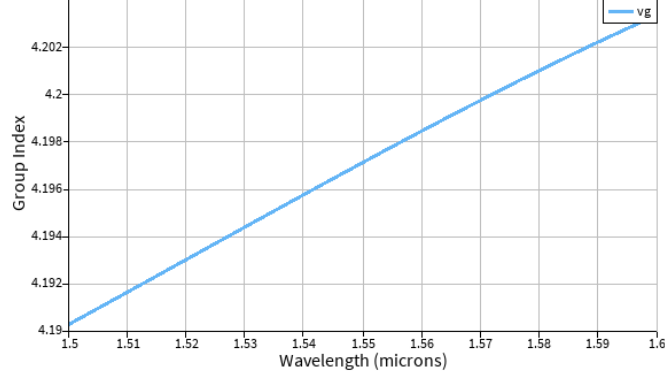
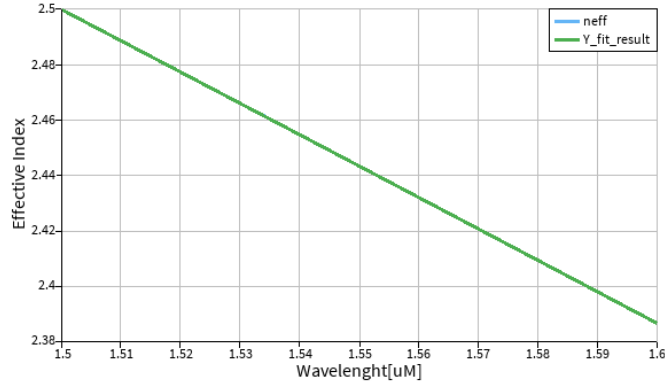Fig. 2. Simulated group index n_g versus wavelength for the 500 nm-wide TE strip waveguide

Fig. 3. Simulated effective index n_{eff} and group index n_g versus wavelength for the 500 nm-wide TE strip waveguide, along with a polynomial compact model fit.

TABLE I

MZI DESIGN VARIANTS AND EXPECTED FREE SPECTRAL RANGE AT $\lambda_0 = 1550\,\text{nm}$, WITH $n_g(\lambda_0) = 4.197$.

Design ID	ΔL (μm)	Polarization	Est. FSR (nm)
MZI_TE_W500_DL30	30	TE	19.08
MZI_TE_W500_DL50	50	TE	11.45
MZI_TE_W500_DL100	100	TE	5.72
MZI_TE_W500_DL50_A	50	TE	11.45
MZI_TE_W500_DL50_B	50	TE	11.45

Figure 4 shows a simulated spectrum for MZI_TE_W500_DL30, illustrating a relatively large FSR across the available wavelength range. Figure 5 and Figure 6 shows the spectrum for MZI_TE_W500_DL50 and MZI_TE_W500_DL100 respectively, demonstrating the reduction in FSR as ΔL increases.

The FSR from these simulated spectra were used with (15) to obtain the group index.

IV. CONCLUSION

This proposal presented a set of silicon strip waveguide Mach–Zehnder interferometers using a 500 nm $\times$ 220 nm quasi-TE waveguide with several path length differences ΔL. A compact model for the effective and group indices was developed from mode simulations and used with an analytical MZI transfer function to predict transmission spectra and free spectral ranges. The simulation of different MZI implementations shows simulated behavior as expected.
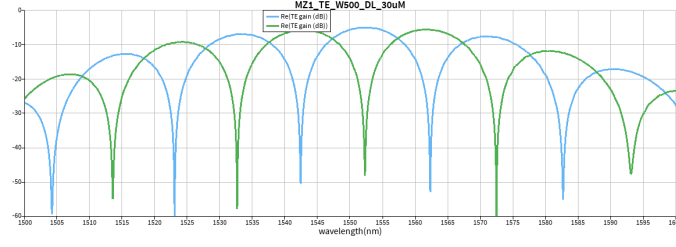
Fig. 4. Simulated transmission spectrum for MZI_TE_W500_DL30, showing a relatively large free spectral range.
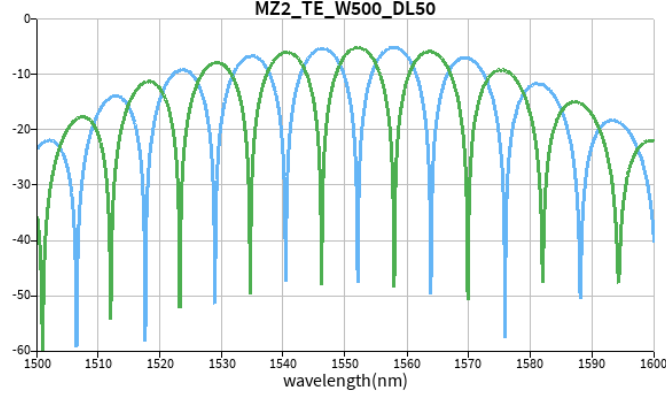

Fig. 5. Simulated transmission spectrum for MZI_TE_W500_DL50, showing a reduced free spectral range due to the larger path length difference.
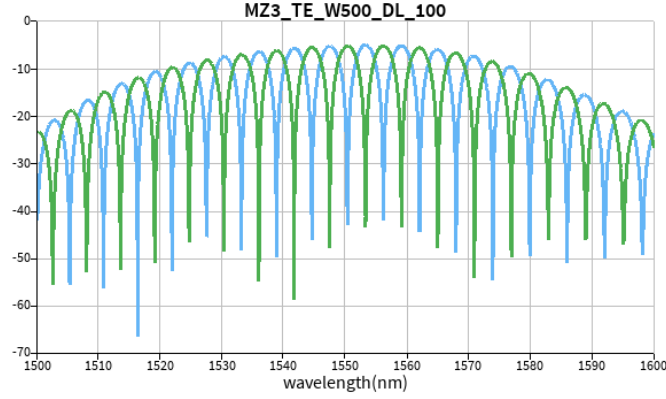

Fig. 6. Simulated transmission spectrum for MZI_TE_W500_DL100, showing a further reduced free spectral range due to the larger path length difference.

REFERENCES

[1] L. Chrostowski and M. Hochberg, *Silicon Photonics Design: From Devices to Systems*. Cambridge, U.K.: Cambridge Univ. Press, 2015.

[2] B. E. A. Saleh and M. C. Teich, *Fundamentals of Photonics*, 2nd ed. Hoboken, NJ, USA: Wiley, 2007.

[3] A. Yariv and P. Yeh, *Photonics: Optical Electronics in Modern Communications*, 6th ed. New York, NY, USA: Oxford Univ. Press, 2007.

[4] W. Bogaerts and L. Chrostowski, "Silicon photonics circuit design: Methods, tools and challenges," *Laser & Photonics Reviews*, vol. 12, no. 4, p. 1700237, 2018.

[5] Ansys Lumerical MODE software, https://www.ansys.com/products/optics/ansys-lumerical-mode

[6] Ansys Lumerical INTERCONNECT software, https://www.ansys.com/products/optics/ansys-lumerical-interconnect